Synthesis of Europium Oxide Nanorods by Ultrasound Irradiation

V. G. Pol,[†] O. Palchik,[†] A. Gedanken,*[,†] and I. Felner[‡]

Department of Chemistry, Bar-Ilan University, Ramat-Gan 52900, Israel, and The Racah Institute of Physics, The Hebrew University, Jerusalem 91904, Israel

Received: March 31, 2002; In Final Form: June 6, 2002

Europium oxide nanorods have been prepared by the sonication of an aqueous solution of europium nitrate in the presence of ammonia. The properties of the Eu_2O_3 nanorods were characterized by X-ray diffraction, thermogravimetric analysis, differential scanning calorimetry, Mössbauer spectroscopy, transmission electron microscopy, high-resolution transmission electron microscopy, high-resolution scanning electron microscopy, and X-ray photoelectron spectroscopy. The particle sizes measured from transmission electron micrographs and HRSEM are about 50 × 500 nm ($W \times L$). A possible sonochemical mechanism for formation of the europium oxide nanorods is discussed.

Introduction

The science and technology of nanomaterials has created great excitement and expectations in the past few years. By its very nature, the subject is of immense academic interest, having to do with very tiny objects in the nanometer regime. There has already been much progress in the synthesis, assembly, and fabrication of nanomaterials (nanocrystals, nanowires, nanotubes, nanorods, nanoflasks, nanospheres) and, equally important, in the potential applications of these materials in the wide variety of technologies.[1] Chemists are increasingly concerned with the synthesis, structure, enhanced properties, and simulation of advanced or novel materials. The use of the inorganic−organic interface to achieve shape-controlled synthesis of inorganic materials is an emerging soft chemical route.[2]

A considerable number of studies has been reported on the bulk synthesis of nanowires or nanorods [i.e., nanorods synthesis of TiO_2 by sol−gel,[3] MgO by heating,[4] Sb_2O_3 by microemulsion,[5] scission−template−transportation route[6] to $CdIn_2S_4$, solvothermal azide decomposition route[7] to form GaN, Bi_2S_3 by microwave irradiation,[8] Bi_2S_3 by hydrothermal synthesis,[9] gold nanorods capped with cationic surfactants in water,[10] SnO_2 by redox reaction,[11] electrophoretic growth of lead zirconate titanate nanorods,[12] silver nanorods by electrochemical[13] method, and by the growth of the nanoparticles, CdSe nanorods were formed with high aspect ratio,[14] etc.] However, complicated apparatus, complex process control, and special conditions are required for these approches.

A sonochemical approach was used to prepare a variety of nanoregime materials such as magnetite nanorods of aqueous iron(II) acetate in the presence of β-cyclodextrin.[15] Lanthanum carbonate particles, which can be used as a precursor for needle-shaped lanthanum oxide, have been synthesized from lanthanum nitrate and urea.[16] Elongated needles[17] of $In(OH)_3$ and Pb(OH)-Br have also been prepared by an ultrasonic method in the presence of a cationic surfactant, cetyltrimethylammonium bromide.[18]

Rare earth ions (Re^{3+}) are particularly suitable for applications as light emitters due to their well-defined transitions within the 4f shell. The synthesis of nanocrystalline Eu_2O_3 can be accomplished by a number of processes, including sol−gel techniques,[19] gas-phase condensation,[20] colloidal chemical method,[21,22] and sonochemical techniques.[23] In this paper we report a novel sonochemical reaction which produces dispersed nanorods of Eu_2O_3.

Experimental Section

Sonochemical Synthesis of Europium Oxide Nanorods. A 500 mg amount of europium nitrate pentahydrate (Aldrich) were dissolved in 100 mL of distilled water in a sonication cell, and the cell was attached to the sonicator horn. A clear solution was sonicated with high-intensity ultrasound radiation for 120 min at a constant temperature of 15−20 °C (Sonics and Materials VCX 600 sonifier, 20 kHz, 40 W/cm^2). The reaction was maintained at pH 8 by dropwise addition of 10−12 mL of 24% (wt) aqueous ammonia during the sonication. The precipitate was formed gradually during the dropwise addition of ammonia. The product was washed three times with doubly distilled water, centrifuged, and dried under a vacuum at room temperature. A control reaction was also conducted when a total of 10 mL of ammonia was added at once at the beginning of the reaction and without pH control. The reaction was also carried out as above with pH and temperature control, but with NaOH, instead of ammonium hydroxide. The precipitates of all above-mentioned reactions was dried under vacuum and referred to "as-prepared samples" synthesized by sonochemical method. Crystallization of the as-prepared samples was carried out by heating a small amount of the sample in a boat crucible at a temperature of 700 °C for 4 h in air.

A reaction was also carried out under microwave irradiation. Immediately after mixing the reactants (including 10 mL of ammonia), the solution was placed in a microwave refluxing system for 30 min with power 60% without further addition of ammonia. At the end of the reaction the gray precipitate was centrifuged, washed repeatedly with distilled water, and dried under vacuum. These products will be referred to as-prepared sample assisted by the microwave method.

* To whom all correspondence should be addressed. Fax: +972-3-5351250. E-mail: gedanken@mail.biu.ac.il.
† Bar-Ilan University.
‡ The Hebrew University.

10.1021/jp025864g CCC: $22.00
Published on Web 08/13/2002

TABLE 1: Experimental Conditions for the Preparation of the Samples[a]

					XRD product		
sample	reagents	sono./MW	pH	ammonia addition	AP	H	morphology TEM/SEM
1	$Eu_2(NO_3)_3$	sono.	8 (const)	10−12 mL (during reacn)	A	C	nanorods
2	$Eu_2(NO_3)_3$	sono.	9.3 (initial)	10 mL at the beginning	A	C	small amount of nanorods
3	$Eu_2(NO_3)_3$ + NaOH	sono.	8 (const)	−	A	C	nanoparticles
4	$Eu_2(NO_3)_3$	sono.	6.3	−	--	--	no product
5	$Eu_2(NO_3)_3$	MW	9.3 (initial)	10 mL at the beginning	C	C	nanoparticles

[a] AP = as-prepared; H = heated (heated at 700 °C, 4 h, in air); A = amorphous; C = crystalline; sono. = sonochemical; MW = microwave irradiation.

Table 1 summarizes the various conditions under which the reactions were conducted. An additional reaction was carried out with vigorous mixing, but without sonication or microwave irradiation only micrometer-sized particles formed, and no nanorods.

Characterization. The powder X-ray diffraction patterns of the product were measured with a Bruker AXS D* advanced powder X-ray diffractometer (using Cu K_α = 1.5418 Å radiation). The product morphology, particle size, chemical composition, and crystalline phases were studied with transmission electron microscopy (TEM), scanning electron microscopy, and high-resolution TEM. The TEM characterization was done on a JEOL−JEM 1010 SX microscope, working at a 100 kV accelerating voltage. Samples for the TEM experiments were prepared by suspending the dried sample in absolute ethanol in a sonication bath for 20 min. A drop of the sample suspension was allowed to dry on a copper grid (400 mesh, Electro Microscopy Sciences) coated with a carbon film. High-resolution scanning electron micrographs (HRSEM) were obtained using an LEO Gemini 982 field emission gun SEM (FEG-SEM) operating at a 4 kV accelerating voltage. High-resolution transmission electron micrographs (HRTEM were obtained using a JEOL-3010 set to a 300 kV accelerating voltage. A conventional CCD video camera, with spatial resolution of 768 × 512 pixels, was used to digitize the micrographs, which were then processed using Digital Micrograph software. Mössbauer spectroscopy (MS) studies were carried out at 300 K using a conventional constant acceleration spectrometer. The ^{151}Eu MS were measured with a mCi $^{151}Sm_2O_3$ source, and a least-squares fit was applied to the spectra assuming a splitting of the source. Thermogravimetric analysis was carried out under a stream of nitrogen, at a heating rate of 3 °C/min using a Mettler TGA/STDA 851. Differential scanning calorimetric (DSC) analysis of the sample in a crimped aluminum crucible was carried out up to a temperature of 550 °C, using a Mettler DSC-301 under a stream of nitrogen, at a heating rate of 3 °C/min. X-ray photoelectron spectra (XPS) were measured with an AXIS, HIS 165, Kratos Analytical, ULTRA.

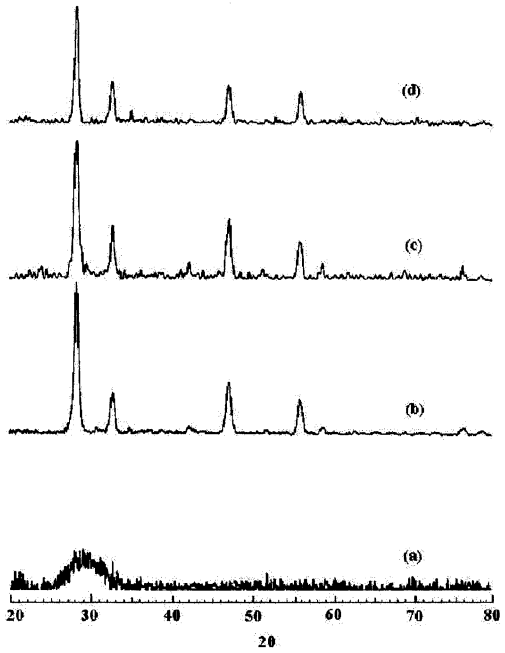

Figure 1. X-ray diffraction patterns of sonochemically synthesized (a) as-prepared amorphous sample, (b) sample 1 heated at 700 °C for 4 h, (c) sample 2 heated at 700 °C for 4 h, and (d) sample 3 heated at 700 °C for 4 h. (All samples were heated in air.)

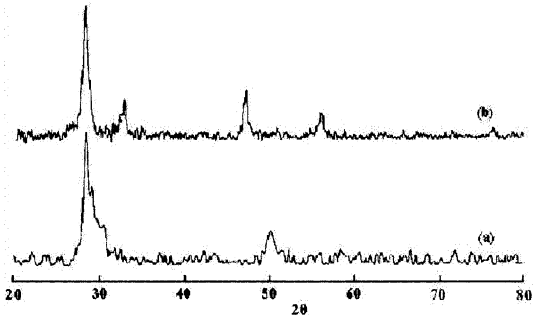

Figure 2. X-ray diffraction patterns of microwave-assisted (a) as-prepared sample (sample 5) and (b) sample 5 heated at 700 °C, for 4 h in air.

Results and Discussion

X-ray Diffraction Studies. The phase identification of all the products was performed by powder X-ray diffraction (XRD). The sonochemically synthesized as-prepared samples (1−3) were amorphous. Only the microwave-assisted as-prepared sample 5 was crystalline. Figure 1a shows the X-ray diffraction pattern of one of the ultrasonically synthesized as-prepared amorphous samples (sample 1). The amorphous nature of the sample is demonstrated by the absence of any diffraction peaks. After being heated to 700 °C for 4 h in air, all the amorphous samples crystallized. Parts b−d of Figure 1 show the powder XRD patterns of all the heated samples (samples 1−3, respectively). All these crystalline patterns were indexed as a body centered cubic Eu_2O_3, and the calculated lattice parameters were in agreement with the PDF database values (PDF No. 34−0392). No peaks characteristic of any impurities were observed. The PXRD patterns of the as-prepared microwave-assisted sample (sample 5) and the same heated sample (to 700 °C, 4 h) are shown in Figure 2a,b. In this case the pattern in Figure 2a was identified as $Eu(OH)_3$ (PDF No. 83−2305) and the pattern in Figure 2b as Eu_2O_3 (PDF No. 34−0392). The characterization of the sonochemical as-prepared amorphous products was aided by other measurements such as TGA, DSC, XPS, and MS.

Themogravimetric and Differential Scanning Calorimetric Measurements. Thermogravimetric analysis (TGA) was used in order to find out the chemical nature (europium oxide or

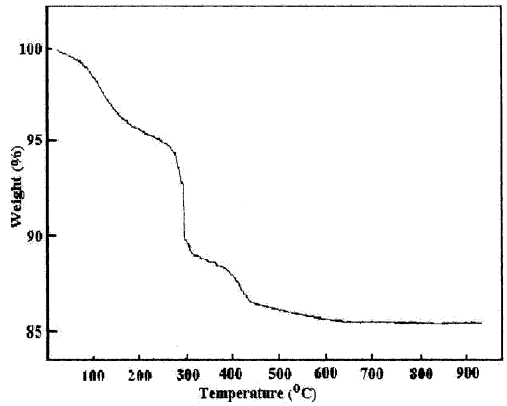

Figure 3. Thermogravimetric analysis plot of as-prepared europium hydroxide (sample 1) synthesized by the sonochemical method.

hydroxide) of the sonochemically synthesized as-prepared amorphous compound. When thermogravimetric analysis of europium hydroxide nanorods was initially carried out under a stream of nitrogen at a heating rate of 10 °C/min., weight loss was observed in only one step. To study the multistep weight loss, the thermogravimetric analysis was carried out under a flowing stream of nitrogen at a heating rate of 3 °C/min. The TGA pattern of the as-prepared product showed a total weight loss of 14.5% over the temperature range of 80−600 °C. The weight loss occurred in three steps (Figure 3). We could explain this result as a decomposition of the $Eu(OH)_3$ as shown in eqs 1 and 2.

$$2Eu(OH)_3 \rightarrow 2EuOOH + 2H_2O \quad (1)$$

$$2EuOOH \rightarrow Eu_2O_3 + H_2O \quad (2)$$

The decomposition starts at 80 °C and continues up to 600 °C. The first decomposition of the as-prepared sample, which took place at 100 °C, is attributed to the desorption of water molecules from the surface of the nanorods. The second decomposition occurred at 300 °C. The overall weight loss observed in the first two decomposition steps was 10% compared with a theoretical weight loss of 8.9% for the conversion of $Eu(OH)_3$ to EuOOH. Above 340 °C, the tranformation of EuOOH to Eu_2O_3 sets in and it is completed at 600 °C. The observed weight loss for this step was 4.5% compared with a theoretical weight loss of 5.6% for the conversion of EuOOH to Eu_2O_3. The total observed weight loss was 14.5%, compared with a theoretical weight loss of 15.3% for the loss of three water molecules. TGA data are in good agreement with the data reported by Shyama.[24] The end product of TGA measurement was found to be pure Eu_2O_3, as inferred from the XRD results.

The differential scanning calorimetric pattern of the as-prepared sample (Figure 4) showed a very broad endotherm at about 100 °C, which is attributed to the loss of surface water molecules from the nanorods. The second strong endotherm occurred at about 310 °C and is attributed to the decomposition of europium hydroxide and formation of oxy−hydroxide. The third broad endotherm at about 436 °C is attributed to the decomposition of EuOOH into Eu_2O_3. In our DSC study we could not see any exothermic peak that can be attributed to the crystallization of the sample. This may be explained as follows. The sample which was heated at 450 °C shows an amorphous nature, while the sample heated at 500 °C shows a crystalline nature, as identified by XRD patterns. The broad strong endotherm at about 440 °C therefore masks the exotherm above

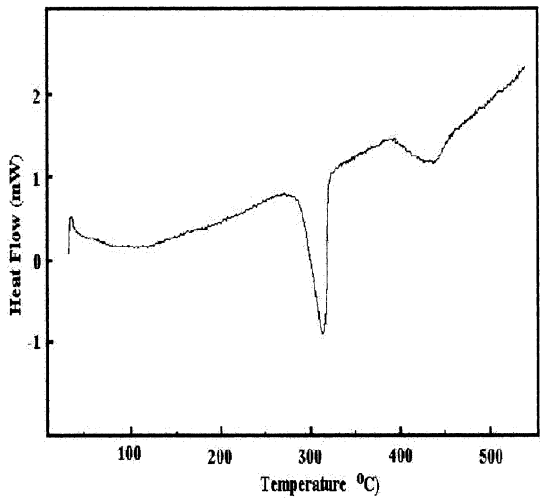

Figure 4. DSC plot of as-prepared europium hydroxide (sample 1) synthesized by the sonochemical method.

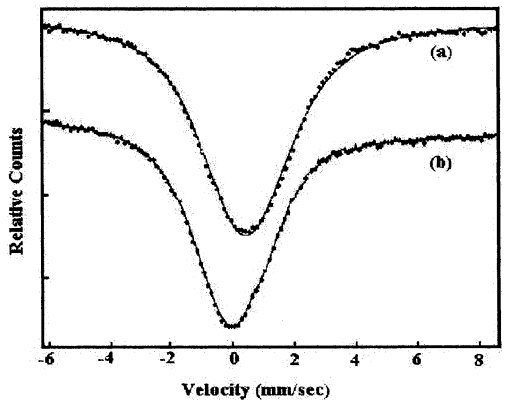

Figure 5. ^{151}Eu Mössbauer spectrum of (a) sample 1 heated at 700 °C for 4 h and (b) as-prepared sample 1.

450 °C. The cooling and second heating cycle is featureless (not shown here). In summary, the DSC and TGA data are in good agreement and support the three step decomposition mechanism proposed above.

Mössbauer Spectroscopy Measurements. To support our proposal that the sonochemically amorphous product formed is europium hydroxide, Mössbauer spectroscopy (MS) was performed. On the basis of MS, it is possible to distinguish europium oxide from the hydroxide and to determine the oxidation state of the europium. Figure 5 shows the ^{151}Eu Mössbauer spectra of the as-prepared and heated samples of europium hydroxide (sample 1). The hyperfine parameters obtained for the as-prepared sample are as follows: (i) line width (W) = 1.92 mm/s, (ii) isomer shift (IS) = −0.065 mm/s, and (iii) quadrupole splitting (QS) = − 2.47. The hyperfine parameters obtained for the magnetic subspectrum of the 700 °C calcinated sample are as follows: (i) W = 2.52 mm/s, (ii) IS = 0.34 mm/s, and (iii) QS = −2.66. The heated sample shows the same hyperfine parameters as those of a commercial sample of pure Eu_2O_3. The as-prepared sample shows a broad single line and has negative isomer shift, indicating that this compound is more ionic than the Eu_2O_3. Its IS is in good agreement with previously reported MS data[25] for $Eu(OH)_3$.

On the basis of XRD, TGA, DSC, and MS data, we conclude that the amorphous sonochemical product formed is europium hydroxide and that it transforms upon heating to crystalline Eu_2O_3.

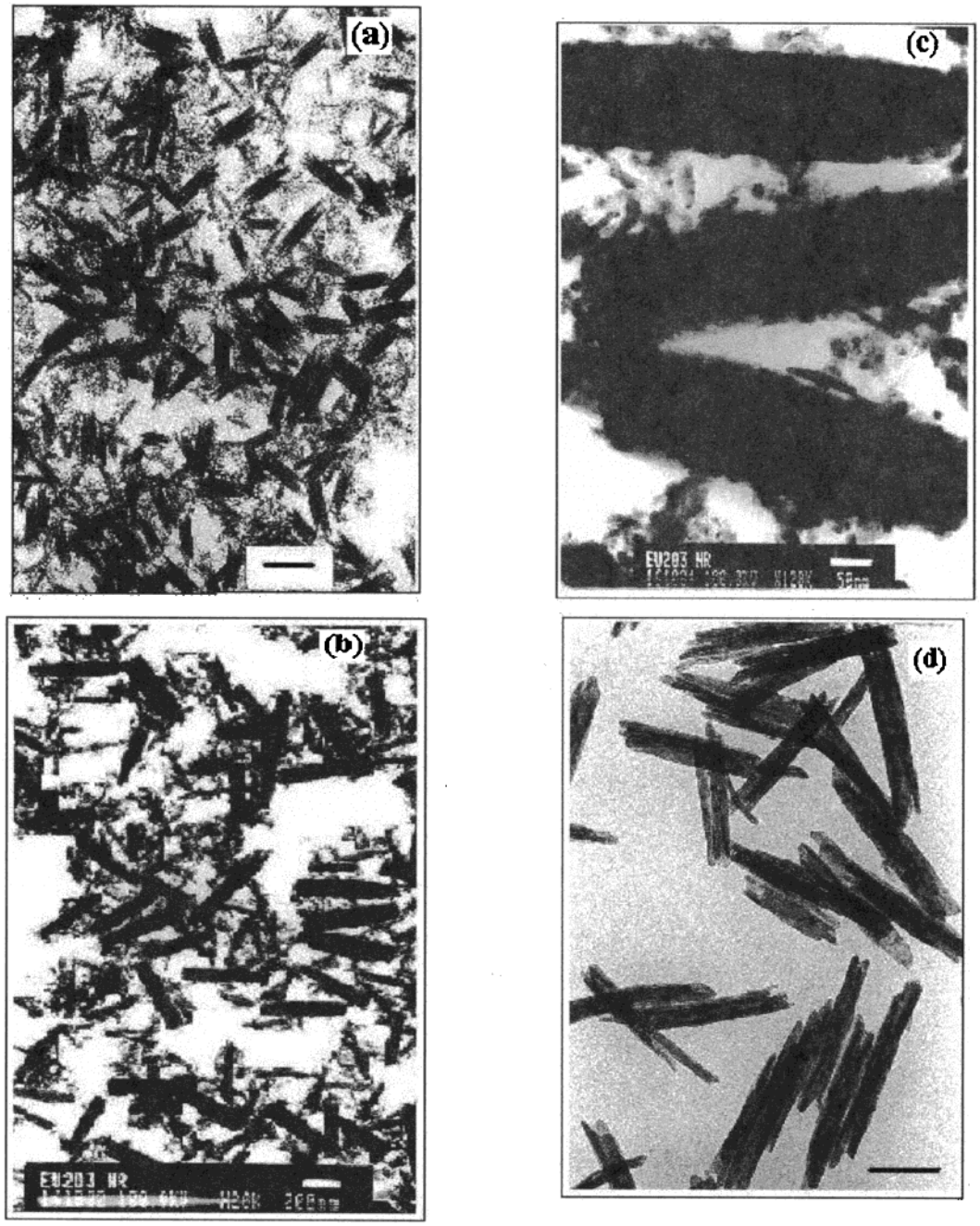

Figure 6. TEMs of (a) the sonochemically synthesized europium hydoxide nanorods after 60 min of sonication (bar equals 100 nm), (b) europium hydroxide after 120 min of sonication, (c) europium hydroxide nanorods at higher resolution, and (d) europium hydoxide nanorods after bringing the colloidal solution to pH 8 by addition of aqueous ammonia and sonicating for 1 h (bar equals 200 nm).

Electron Microscopy Studies. To study the size, size distribution, and morphology of the as-prepared and annealed compounds, TEM, HRSEM, and HRTEM measurements were conducted. TEM micrographs of the as-prepared and the annealed samples were found to be identical. TEM images of the sonochemically as-prepared products identified as europium hydroxide, as shown in Figure 6a, demonstrate that the morphology of the as-prepared products is that of nanorods. The size distribution is narrow, most of the nanorods having a width of 50 nm and a length of ~500 nm. Figure 6b shows the TEM micograph of the as-prepared product annealed at 700 °C. The shape of the as-prepared material is unchanged upon heating, implying that the nanorods are neither damaged, nor destroyed, nor formed during annealing at 700 °C.

It is important to note that, in addition to the rods, a few nanoparticles are also observed. Some particles of 5−10 nm diameter can be detected which are attached to the surface of the rods. Figure 6c shows Eu_2O_3 nanoparticles attached with different orientations, indicating that the rods may be growing from the small nanoparticles. To test this possibility, we carried out a shorter experiment in which the original solution was sonicated for only 30 min. This led to formation of 5−10 nm nanoparticles as the sole product. No rods were observed under these conditions. Sonication times of longer than 30 min led to the growth of the nanoparticles eventually forming the nanorods. After 30−60 min of sonication, nanorods of 15−25 nm width and ~125 nm length were observed (Figure 6a). Extending the sonication time from 60 to 120 min induced further growth of nanorods to 50 × 500 nm. The rods did not grow further when the sonication continued for up to a total of 5 h (Figure 6b). To test our conjecture that consumption of the nanoparticles causes growth of the rods to halt, we carried out a reaction in which

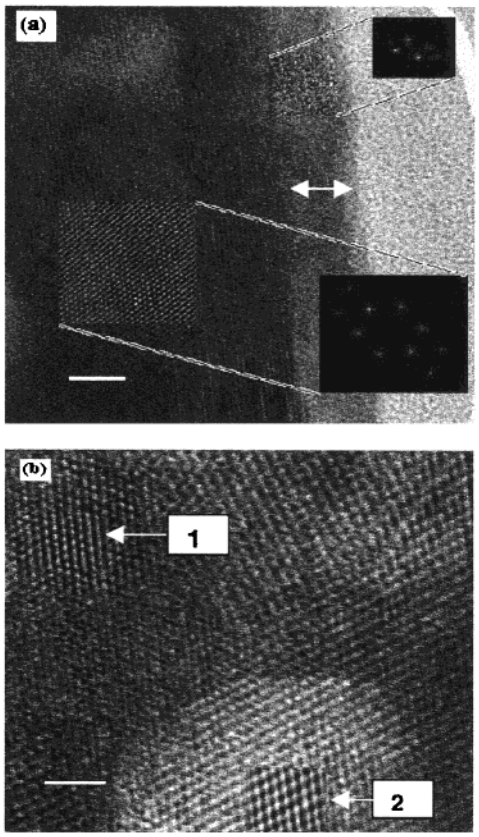

Figure 7. (a) High-resolution transmission electron micrograph of europium oxide nanorods showing partly amorphous surface layer. The double arrow indicates a semicrystalline layer. The insert fast Fourier trasform diffraction patterns of the selected HRTEM area (bar equals 2 nm), and (b) high-resolution TEM of nanoparticles of europium oxide showing different orientations of nanorods (bar equals 2 nm). The particles marked with arrows 1 and 2 are oriented in the [420] and [400] directions, respectively.

after 2 h of sonication more starting material of the same composition was added and sonication continued for another 2 h. This resulted in formation of new nanorods and not the growth of the original rods. The new nanorods are have the same aspect ratio as sample 1. A control reaction in which only europium nitrate was sonicated resulted in no products. When this colloidal solution was brought to pH 8 by the addition of aqueous ammonia and sonicated for 1 h, only nanorods similar to sample 1 were obtained. Nanoparticles were not detected under these conditions (Figure 6d).

The nature of the product as a rod and not a tube is deduced from HRTEM measurements. The HRTEM image of calcinated sample 1 is shown in Figure 7. It is possible to see that the nanorods are indeed built from nanoparticles. This can be seen from the zone axis of the individual particles pointing in different directions. The fringes marked by the arrow 1 in Figure 7b are oriented along the [420] plane. The calculated interplanar distance is 0.245 nm. The fringes marked by arrow 2 in Figure 7b are oriented along the [400] plane, and the calculated interplanar distance is 0.273 nm. The orientation of the planes and their calculated interplanar distances are close to the XRD data (PDF No. 34-0392). The particles are formed as the sonication products are pushed against each other as a result of the microjets created when the bubble collapses. It is well-known that the speeds at which these particles are projected can cause melting at the contact area when they collide.[26a,b] The rods are created as a result of their collisions.

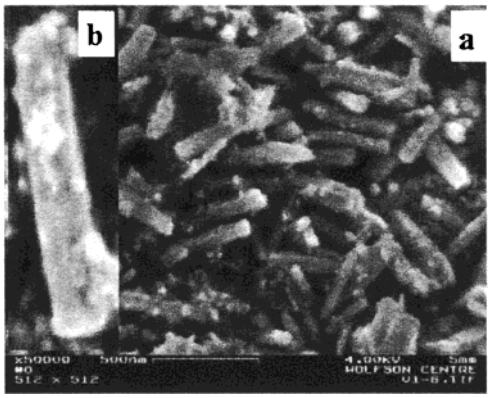

Figure 8. HRSEM of (a) europium oxide nanorods and (b) a single nanorod of europium oxide (50 × 500 nm) at higher resolution.

The fast Fourier transform electron diffraction patterns made from the different parts of the rod (heated sample, Eu_2O_3) substantiate our interpretation since they also show that the Eu_2O_3 rods are build from Eu_2O_3 particles with different orientations (Figure 7b). This mechanism is based on the assumption that the nanoparticles annealed at 700 °C undergo crystallization. This is reflected also in the shape of the rod which is unchanged when annealed at 700 °C for 4 h. The HRTEM picture shows that the outer shells of many nanorods are partly crystalline and partly amorphous. The thickness of this shell is approximately 1−3 nm (Figure 7a). The HRSEM micrograph of the annealed sample is shown in Figure 8a,b. Nanorods are seen to be the main component on the grid. The insert shows a single nanorod of europium oxide at higher resolution (Figure 8b). In this picture, as well as in the TEM image, nanoparticles are observed glued to the surface of the nanorods. Small numbers of nanoparticles were also be detected unattached to the rods. The diameter of the "glued" nanoparticles is 5−10 nm, similar to what is observed in the low-resolution TEM.

The sample prepared by microwave irradiation does not show any rodlike structure but rather the small ribbonlike structure of the europium hydroxide. From this experiment we can further conclude that the microwave synthesis lacks the sintering effect of the microjets formed after the collapse of the bubble in the sonochemical process.

XPS Measurements. X-ray photoelectron spectroscopy (XPS) is known to probe only the surface of the particles. The analysis of low-energy electrons, which are strongly scatterened in materials and consequently have a small escape depth, enables information to be obtained from the top few atomic layers of a surface. In XPS, excitation by X-rays allows core atomic levels to be probed and the resultant chemical shift provides an indication of the oxidation state of the material in the surface. XPS also provides more evidence for the purity and composition of the nanorods. Parts a and b of Figure 9 show the binding energies of Eu $3d_{5/2}$ for the as-prepared and annealed samples. Carbon is always present in XPS as a result of hydrocarbon deposits in air and/or under vacuum, which is commonly used as an internal energy calibrant at 285.0 eV binding energy. The as-prepared material showed binding energies for the Eu $3d_{5/2}$ and Eu $3d_{3/2}$ of 1133.3 and 1161.7 eV, respectively. In the annealed sample the binding energies for Eu $3d_{5/2}$ and Eu $3d_{3/2}$ were 1134.3 and 1162.7 eV, respectively. The small satellite peaks observed at 1154.9 and 1126.7 eV correspond to a Eu oxidation state of +2. This is probably due to Eu ions surrounded by a highly disturbed coordination. This result is in agreement with HRTEM measurements (Figure 7a) in which a

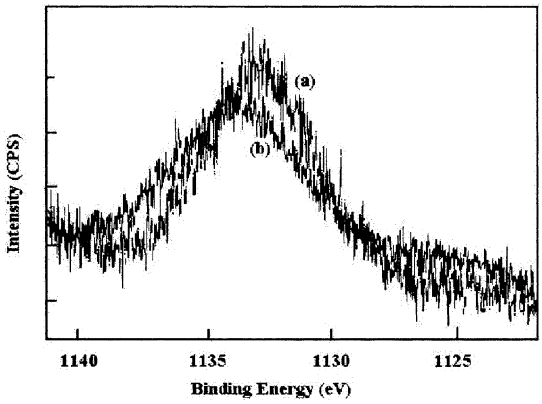

Figure 9. X-ray photoelectron spectrum of Eu $3d_{5/2}$ (a) as-prepared europium hydroxide (sample 1) and (b) sample 1 heated at 700 °C for 4 h.

semicrystalline shell surrounding many nanorods was observed. The binding energies are consistent with the energies observed in previously published XPS spectrum of this compound.[27] The composition of the surface area of the calcinated compound calculated on the basis of XPS data displays the Eu:O ratio of 1:1.22 compared with the theoretical value of 2:3 for Eu_2O_3. Thus, even though XPS is a surface method of analysis and penetrates only to a depth of 1−5 nm, it still yields a composition for the Eu_2O_3 nanorods close to the bulk composition. A small XPS peak assigned to the presence of nitrogen is also observed in the as-prepared material. This is due to the adsorption of NH_4OH molecules on the surface. The peak disappears in the annealed sample.

Sonochemical Mechanism for Formation of the Europium Oxide Nanorods. Addition of alkali to a solution of a europium salt yields the hydroxide. Amines as well as ammonia are also sufficiently basic to precipitate hydroxides of the most rare earth trivalent ions.[24] Sonication of an aqueous solution of europium nitrate in the presence of ammonia results in the precipitation of europium hydroxide:

$$Eu^{3+}(aq) + 3H_2O \xrightarrow[\text{aq ammonia}]{)))))))} Eu(OH)_{3\,(s)} + 3H^+(aq) + NH_4^+(aq)$$

The as-prepared material is europium hydroxide as confirmed by TGA, DSC, XPS, and Mössbauer spectroscopy measurements as well as by PXRD of the as-prepared sample assisted by microwave irradiation. The presence of ammonium ion seems to be important for the formation of particles with morphology usually obtained in the absence of ammonia. In our case this was confirmed by the absence of precipitate after sonicating a solution of europium nitrate without addition of ammonia. Regarding the shape of the as-prepared product, careful examination of TEM, HRSEM, and HRTEM micrographs reveals that the rod-shaped particles of europium hydroxide consist of a few spherical particles aligned in one direction.

The formation of europium hydroxide nanorods may be explained as follows. The $Eu(OH)_3$ particles formed upon collapse of the bubbles adsorb NH_4^+ ions or ammonia on their surfaces, thus forming a monolayer and fusing them by hydrogen bonding. In this way ammonium ions would be responsible for the observed morphology. This adsorption of NH_4^+ on the surface of the particles is supported by the results of Sherif et al.,[28] who showed that ammonium nitrate (NH_4NO_3) is adsorbed on the surface of the powder after precipitation. Wang et al.[29] also concluded that NH_4Cl is adsorbed onto the surface of the particles, due to the high surface energy associated with the nanophase rod shaped materials. In the case of homogeneous liquid-phase systems, the generated bubbles collapse symmetrically. But, considering a system where solid particles are also present, as it is in the present case, then an asymmetric collapse will occur. This mode of collapse results in the generation of high-speed microjets,[30,31] the velocity of which may be very high. Due to this very high velocity of liquid jets the $Eu(OH)_3$ nanoparticles are pushed toward each other, forming the nanorods. The special effect of the ultrasound radiation is demonstrated in the hydrolysis reaction, which leads to the formation of a nanoproduct that later forms nanorods. In contrast, the "still" reaction yields only micrometer-sized particles of the same product.

Conclusions

Europium hydroxide nanorods have been prepared by sonication of an aqueous solution of europium nitrate in the presence of ammonia. The sizes of the nanorod measured from transmission electron micrographs and HRSEM are about 50 × 500 nm. XRD, TGA, DSC, and Mössbauer analyses confirm that the sonochemically prepared amorphous compounds transform upon heating to crystalline Eu_2O_3. It has been demonstrated for the first time that sonochemical hydrolysis of Eu^{3+} yields nanorods of Eu_2O_3.

Acknowledgment. V.G.P. is thankful to the President's Fund of Bar-Ilan University, Israel, for financial assistance. The authors would like to thank Y. Gofer for XPS measurements and to Prof. Z. Malik, Department of Life Sciences, for extending the use of TEM and SEM facilities.

References and Notes

(1) Rao, C. N. R.; Cheetham, A. K. *J. Mater. Chem.* **2001**, *11*, 2887.
(2) Mann, S.; Archibald, D. D.; Didymus, J. M.; Douglas, T.; Heywood, B. R.; Meldrum, F. C.; Reeves, M. J. *Science* **1993**, *261*, 1.
(3) Zhang, M.; Bando, Y.; Wada, K. *J. Mater. Sci. Lett.* **2001**, *20*, 167.
(4) Cui, Z.; Meng, G. W.; Huang, W. D.; Wang, G. Z.; Zhang, L. D. *Mater. Res. Bull.* **2000**, *35*, 1653.
(5) Guo, L.; Wu, Z. H.; Liu, T.; Wang, W. D.; Zhu, H. S. *Chem. Phys. Lett.* **2000**, *318*, 49.
(6) Lu, J.; Xie, Y.; Du, G. A.; Jiang, X. C.; Zhu, L. Y.; Wang, X. J.; Qian, Y. T. *J. Mater. Chem.* **2002**, *12*, 103.
(7) Grocholl, L.; Wang, J. J.; Gillan, E. G. *Chem. Mater.* **2001**, *13*, 4290.
(8) Liao, X. H.; Wang, H.; Zhu, J. J.; Chen, H. Y. *Mater. Res. Bull.* **2001**, *36*, 2339.
(9) Shao, M. W.; Mo, M. S.; Cui, Y. Chen, G. Qian, Y. T. *J. Cryst. Growth* **2001**, *233*, 799.
(10) Nikoobakht, B.; El-Sayed, M. A. *Langmuir* **2001**, *17*, 6368.
(11) Liu, Y. K.; Zheng, C. L.; Wang, W. Z.; Zhan, Y. J.; Wang, G. H. *J. Cryst. Growth* **2001**, *233*, 8.
(12) Limmer, S. J.; Seraji, S.; Forbess, M. J.; Wu, Y.; Chou, T. P.; Nguyen, C.; Cao, G. Z. *Adv. Mater.* **2001**, *13*, 1269.
(13) Zhu, J. J.; Liao, X. H. Zhao, X. N.; Chen, H. Y. *Mater. Lett.* **2001**, *49*, 91.
(14) Manna, L.; Scher, E. C.; Alivisatos, A. P. *J Am. Chem. Soc.* **2000**, *122*, 12700.
(15) Kumar, R. V.; Koltypin, Y.; Xu, X. N.; Yeshurun, Y.; Gedanken, A.; Felner, I. *J. Appl. Phys.* **2001**, *89*, 6324.
(16) Jeevanandam, P.; Koltypin, Y.; Palchik, O.; Gedanken, A. *J. Mater. Chem.* **2001**, *11*, 869.
(17) Avivi, S.; Mastai, Y.; Gedanken, A. *Chem. Mater.* **2000**, *12*, 1229.
(18) Jeevanandam, P.; Koltypin, Y.; Mastai, Y.; Gedanken, A. *J. Mater. Chem.* **2000**, *10*, 2143.
(19) Rao, R. P. *J. Electrochem. Soc.* **1996**, *143*, 189.
(20) Bihari, B.; Eilers, H.; Tissue, B. M. *J. Lumin.* **1997**, *75*, 1.
(21) Bhargava, R. N.; Gallagher, D.; Hong, X.; Nurmiko, A. *Phys. Rev. Lett.* **1994**, *72*, 416.
(22) Wakefield, G.; Keron, H. A.; Dobson, P. J.; Hutchison, J. L. *J. Colloid Interface Sci.* **1999**, *215*, 179.
(23) Patra, A; Sominska, E.; Ramesh, S.; Koltypin, Y.; Zhong, Z.; Minti, H.; Reisfeld, R.; Gedanken, A. *J. Phys. Chem. B* **1999**, *103*, 3361.

(24) Shyama P. Sinha, *Europium*; Springer-Verlag: Berlin, Heidelberg, New York, 1967; p 55.

(25) Ross, P. N., Jr.; Delgass, W. N. In *Catalysis*; Hightower, J. W., Ed.; North-Holland: Amsterdam, 1973; p 597.

(26) (a) Henglein, A. *Ultrasonics* **1987**, *25*, 6. (b) Suslick, K. S.; Doktycz, S. J.; Flint, E. B. *Ultrasonics* **1990**, *28*, 280.

(27) Cho, E. J, Oh, S. J. *Phys. Rev. B* **1995**, *59*, 15613.

(28) Sherif. F. G.; Via, F. A. U.S. Pat., 4764357, 1988, to Akzo America Inc.

(29) Wang, L.; Muhammed, M. *J. Mater. Chem.* **1999**, *9*, 2871.

(30) Suslick, K. S. *Ultrasound: Its Chemical, Physical and Biological Effects*; VCH: Weinheim, Germany, 1988.

(31) Doktycz, S. J.; Suslick, K. S. *Science* **1990**, *247*, 1067.